

# Tumor-derived microRNA-494 promotes angiogenesis in non-small cell lung cancer

Guangmei Mao<sup>1</sup> · Yan Liu<sup>1</sup> · Xi Fang<sup>1</sup> · Yahan Liu<sup>1</sup> · Li Fang<sup>1</sup> · Lianjun Lin<sup>2</sup> · Xinmin Liu<sup>2</sup> · Nanping Wang<sup>1,3</sup>

Received: 9 March 2015 / Accepted: 25 May 2015 / Published online: 4 June 2015  
© Springer Science+Business Media Dordrecht 2015

**Abstract** Angiogenesis, a crucial step in tumor growth and metastasis, is regulated by various pro- or anti-angiogenic factors. Recently, microRNAs have been shown to modulate angiogenic processes by modulating the expression of critical angiogenic factors. However, roles of tumor-derived microRNAs in regulating tumor vascularization remain to be elucidated. In this study, we found that delivery of miR-494 into human vascular endothelial cells (ECs) enhanced the EC migration and promoted angiogenesis. The angiogenic effect of miR-494 was mediated by the targeting of PTEN and the subsequent activation of Akt/eNOS pathway. Importantly, co-culture experiments demonstrated that a lung cancer cell line, A549, secreted and delivered miR-494 into ECs via a microvesicle-mediated route. In addition, we found that the expression of miR-494 was induced in the tumor cells in response to hypoxia, likely via a HIF-1 $\alpha$ -mediated mechanism. Furthermore, a specific miR-494 antagomiR effectively inhibited angiogenesis and attenuated the growth of tumor xenografts in nude mice. Taken together, these results demonstrated that miR-494 is a novel tumor-derived paracrine signal to promote angiogenesis and tumor growth under hypoxic condition.

**Keywords** miR-494 · Angiogenesis · Non-small cell lung cancer · Microvesicle

## Introduction

MicroRNAs are a family of non-coding RNAs, ~22 nt in length, which repress gene expression by pairing to the 3'-untranslated regions of target mRNAs [1]. Aberrant expression of microRNAs in tumor cells contributes to tumor growth by the activation of cell proliferation, the induction of resistance to apoptosis and other related pathological process [2]. Using anti-miR oligonucleotides to inhibit onco-miRs has shown efficacies in tumor xenograft models and thus has great potential in cancer therapy [3].

Emerging evidence indicates that miR-494 plays a critical role in cancer development. The level of miR-494 was higher in a number of cancers such as classical Hodgkin's lymphoma [4] and oral squamous cell carcinoma [5]. Anti-miR-494 treatment significantly diminished tumor size in mice with primary myc-driven liver tumor [6]. Recently, it was reported that knockdown of miR-494 in myeloid-derived suppressor cells, one of the most important cell types in tumor microenvironment, inhibited the growth of mouse breast cancer [7], indicating that miR-494 may also promote cancer progression by modulating tumor microenvironment. Angiogenesis is an essential component in microenvironment to tumor growth and metastasis, whereas inhibiting angiogenesis has become a promising strategy for cancer therapy [8]. It has been reported that tumors can promote angiogenesis through different extracellular pathways, including cellular factors and microRNAs [9]. Therefore, we sought to examine a role of miR-494 in the tumor angiogenesis and demonstrated that miR-494 is a novel tumor-derived paracrine

---

**Electronic supplementary material** The online version of this article (doi:10.1007/s10456-015-9474-5) contains supplementary material, which is available to authorized users.

---

✉ Nanping Wang  
nanpingwang2003@yahoo.com

<sup>1</sup> Institute of Cardiovascular Science, Peking University Health Science Center, 38 Xueyuan Rd, Beijing 100191, China

<sup>2</sup> Geriatric Department, Peking University First Hospital, Beijing, China

<sup>3</sup> Cardiovascular Research Center, Xi'an Jiaotong University, Xi'an, China

signal to promote angiogenesis and tumor growth under hypoxic condition.

## Materials and methods

### Cell culture

Human umbilical vein endothelial cells (HUVECs) were cultured as previously described [10, 11]. Tumor cell lines including A549, H1299 and HCC827 were obtained from ATCC and cultured in DMEM supplemented with 10 % fetal bovine serum (FBS) (Invitrogen) [12]. Tumor–endothelial co-culture experiments were performed in six-well plates with 8-micron transwell inserts (BD Biosciences). Tumor cells were seeded in the top inserts with EC monolayers co-cultured in the bottom wells [13, 14]. MicroRNA mimics, inhibitors or mouse full-length HIF-1 $\alpha$  expressing plasmid were transfected with Lipofectamine 2000 (Invitrogen). MicroRNA mimics and inhibitors were synthesized and obtained from GenePharma. Expression of miR-494 and HIF-1 $\alpha$  after transfection were shown in Supplemental Fig. 1D–E.

### Western blotting

Protein samples were extracted from the cells or tumor tissues with lysis buffer (50 mmol/L Tris–HCl, pH 7.5, 15 mmol/L EGTA, 100 mmol/L NaCl, 0.1 % [vol/vol] Triton X-100 and complete protease inhibitor cocktail). Equal amounts of protein were run on 10 % SDS-PAGE and blotted onto polyvinylidene difluoride membranes. The blots were reacted with primary antibodies against HIF-1 $\alpha$  (BD Pharmingen), PTEN (Epitomics), eNOS (BD Pharmingen), phosphorylated (p)-eNOS (S1177), p-Akt (S473) and Akt (Cell Signaling Technology), respectively, followed by the reaction with the appropriate secondary antibodies and the detection with the enhanced chemiluminescence kit as described previously [15].

### Real-time quantitative RT-PCR

Total RNA was isolated from cancer cells and HUVECs using Trizol (Invitrogen), and cDNA was synthesized following standard protocols. Mature miR-494 was quantified by Taqman<sup>®</sup> microRNA Assay (Life Technology) with U6 as control. Real-time PCR involved SYBR Green dye and Taq polymerase. Please see supplemental materials for the primer sequences.

### Chromatin immunoprecipitation assay

Cells were cross-linked with 1 % formaldehyde and quenched before harvest and sonication. The lysates were incubated with 2  $\mu$ g of anti-HIF-1 $\alpha$  antibody or control rabbit IgG, and

then the complexes were precipitated by using protein A/G agarose beads. Immunoprecipitates were extensively washed. DNA was purified by using the QIAGEN PCR purification kit and amplified with the primers flanking the putative HIF-responsive elements (HRE) motifs [16].

### Wound closure assay

Confluent HUVEC monolayers were mechanically wounded with a pipette tip and washed with phosphate-buffered saline (PBS) to remove the debris. The wounded monolayers were cultured in the complete EC medium (M199 supplemented with 20 % FBS, 20 mmol/L HEPES (pH 7.4), 1 ng/mL recombinant human fibroblast growth factor, 90 mg/mL heparin and antibiotics). Wound closure was observed under inverted microscopy, and the images were taken at different time points. Wound closure was measured using softwares and presented as relative distance in pixel (ImageJ) or distance in  $\mu$ m (Leica microscopy imaging software) [17].

### Tube formation

After transfection with miR-494 mimic or inhibitor, HUVECs ( $3 \times 10^4$  cells/well) were seeded onto Matrigel (BD Biosciences). Cells were microscopically recorded for the formation of tube-like structures 16 h later. Data were expressed as the mean  $\pm$  SEM of the tube numbers per field [18].

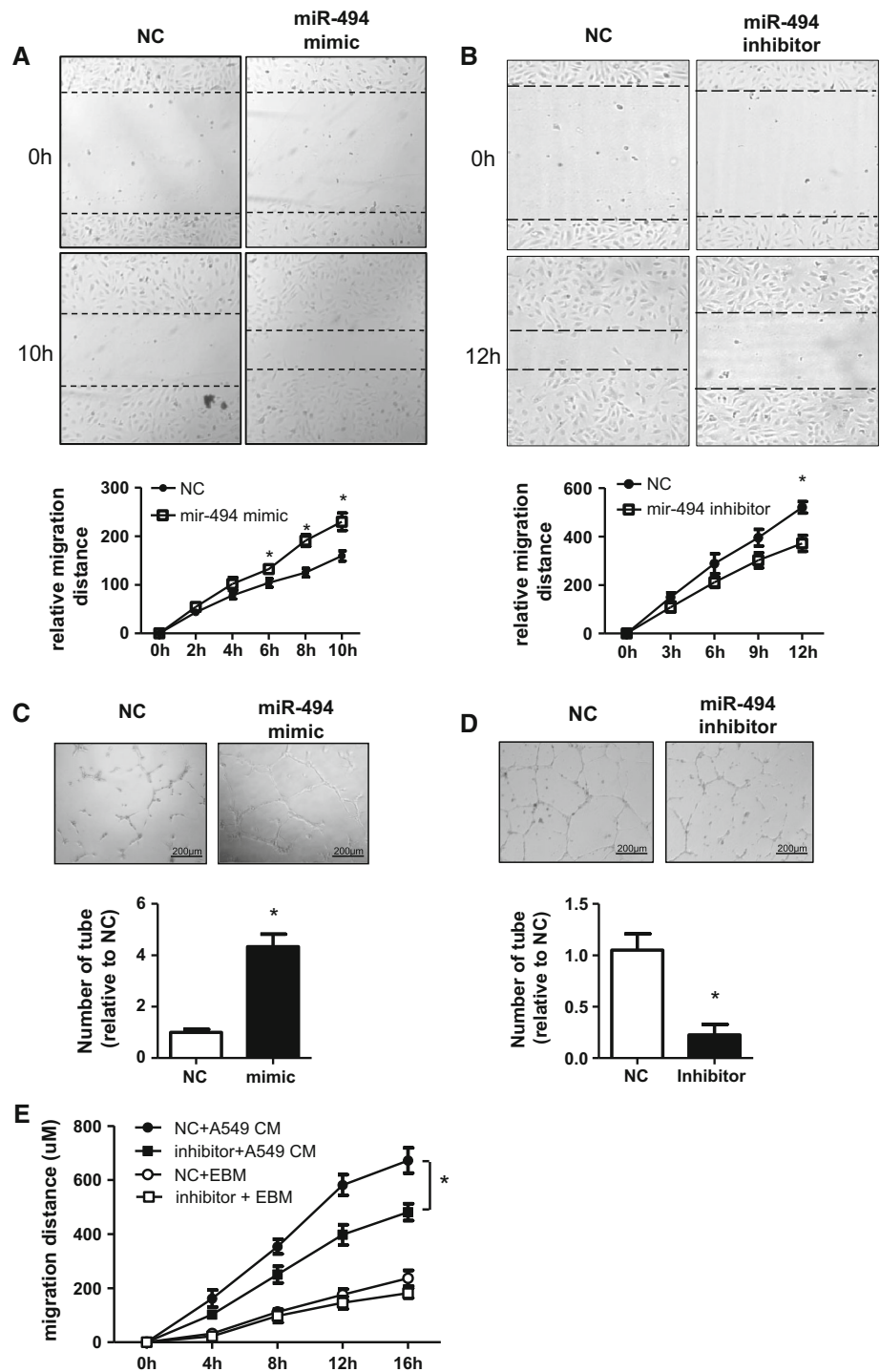
### Microvesicle isolation

Tumor cells were cultured in serum-free DMEM for 48 h. Conditioned medium was collected and centrifuged at 1200g for 3 min to remove living cells and subsequently centrifuged at 14,000g for 10 min to remove cell debris. Supernatants were filtered through a 0.22- $\mu$ m membrane and centrifuged for 30 min at 16,500g. Microvesicles (MVs) were pelleted by ultracentrifugation for 2 h at 110,000g, resuspended in PBS and stored at  $-80$  °C until use [18].

### Mouse model

All procedures involving mouse experiments were approved by the Peking University Animal Care and Use Committee and in conformity with NIH guidelines. Five-week-old male BALB/c nude mice were injected subcutaneously (s.c.) with A549 cells ( $5 \times 10^6$ ) in serum-free RPMI 1640 and Matrigel (v/v 1:1). AntagomiR (GenePharma), which has optimized phosphorothioate modifications to make it more stable than inhibitor, was used in silencing miR-494 in vivo [3]. Control (NC) antagomiR or miR-494 antagomiR (0.2  $\mu$ g) was intratumorally injected twice on the 8th and 15th day. Tumor volume was calculated every 3 days according to width<sup>2</sup>  $\times$  length  $\times$  0.5.

**Fig. 1** miR-494 promoted angiogenesis in vitro. **a** HUVECs were transfected with the miR-494 mimic or scramble control (NC) for 24 h and then subjected to the wound closure assay. Cell migration was assessed by measuring the distances between the migratory edges (*dotted lines*) at different time points after wounding. The unit of relative distance is pixel, measured using ImageJ software. **b** Cells were transfected with the miR-494 inhibitor or scramble control. **c** HUVECs were transfected with miR-494 mimic or scramble control and then seeded on Matrigel. Formation of tube-like structures was counted 16 h later. **d** Cells were transfected with the miR-494 inhibitor or scramble control. *\*P* < 0.05 versus scramble controls (*n* = 3). **e** HUVECs were cultured in serum-free EBM and transfected with miR-494 inhibitor or scramble control before the addition of the A549-conditioned medium (CM). Then, cell migration was assessed at different time points



Mice were killed on the 22nd day. Tumors were removed, weighed and fixed in 4 % paraformaldehyde [19].

**Assessment of tumor angiogenesis**

Tumor specimens were fixed with 4 % paraformaldehyde and embedded in paraffin. Immunohistochemistry was

carried out on 5-μm sections to visualize vascular endothelium by using CD31 antibody (Santa Cruz). Using a Leica DM 4000B photomicroscope (magnification, 100×), six field images were collected from two biopsies per specimen. Any discrete cluster or single cell stained positive for CD31 was counted as one vessel. Tumor vessel density was reported as the average number of vessels number per field [20].

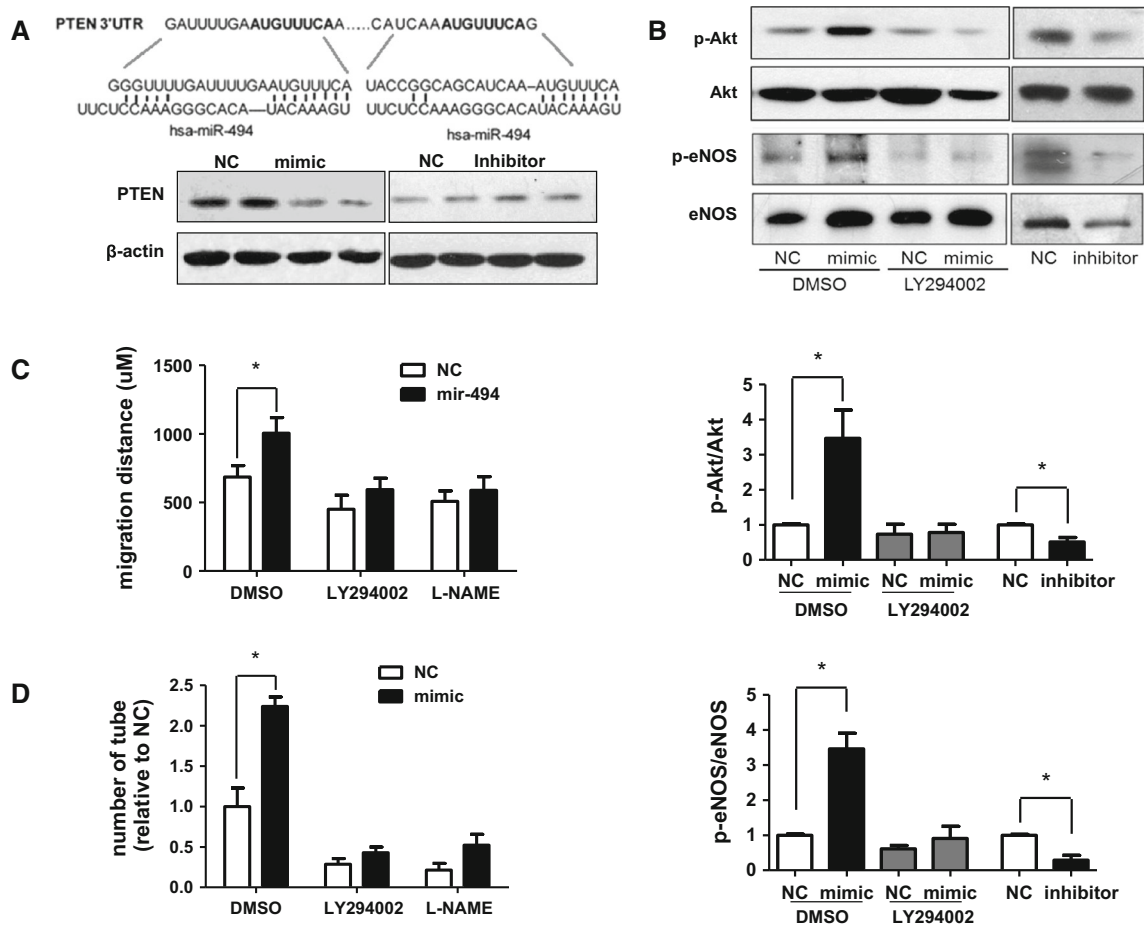


**Fig. 2** Pro-angiogenic effect of miR-494 was mediated by Akt/eNOS pathway. **a** HUVECs were transfected with miR-494 mimic, inhibitor or NC for 24 h. Protein samples were isolated to measure the PTEN level by using western blotting. **b** HUVECs were transfected with miR-494 mimics or NC and maintained in the presence of the PI3K inhibitor LY294002 (50 μM) or vehicle control (DMSO). Alternatively, cells were transfected with miR-494 inhibitor or NC. The levels of phosphorylated Akt and eNOS were detected and shown as fold change in the bar graphs. **c** After transfection with miR-494 or

NC, HUVECs were subjected to the wound closure assay in the presence of LY294002 (50 μM), the eNOS inhibitor L-NAME (100 μM) or DMSO. Cell migration was measured 16 h later. **d** HUVECs were transfected with miR-494 mimic or NC and then seeded on Matrigel in the presence of LY294002, L-NAME or DMSO. Formation of tube-like structure was measured 16 h later. Data presented as mean ± SEM in the bar graph; \* $P < 0.05$  versus NC ( $n = 3$ )

### Statistical analysis

Data were expressed as mean ± SEM. Statistical analyses involved Student's *t* test and one-way analysis of variance (ANOVA). *P* values of <0.05 were considered significant.

## Results

### miR-494 exerts an angiogenic effect in HUVECs

To determine the effect of miR-494 on angiogenesis, we first performed the wound closure experiments in HUVECs transfected with miR-494 mimic, miR-494 inhibitor or their scramble controls (NC). The results showed that miR-494 mimic significantly accelerated the wound closure. In

contrast, miR-494 inhibitor delayed the wound closure (Fig. 1a, b). In addition, the capacity of ECs to form tube-like structures on the Matrigel was increased by the miR-494 mimic and decreased by the miR-494 inhibitor (Fig. 1c, d). These results suggested that miR-494 had a pro-angiogenic activity.

### miR-494 promotes angiogenesis through activation of Akt/eNOS pathway

To further study the mechanism of miR-494 on angiogenesis, we examined the effects of miR-494 on Akt/eNOS pathway, since PTEN, a well-known regulator of Akt pathway, has been reported as a target gene of miR-494 [21]. Firstly, we verified that PTEN was downregulated by miR-494 mimic in HUVECs (Fig. 2a). Then, we examined

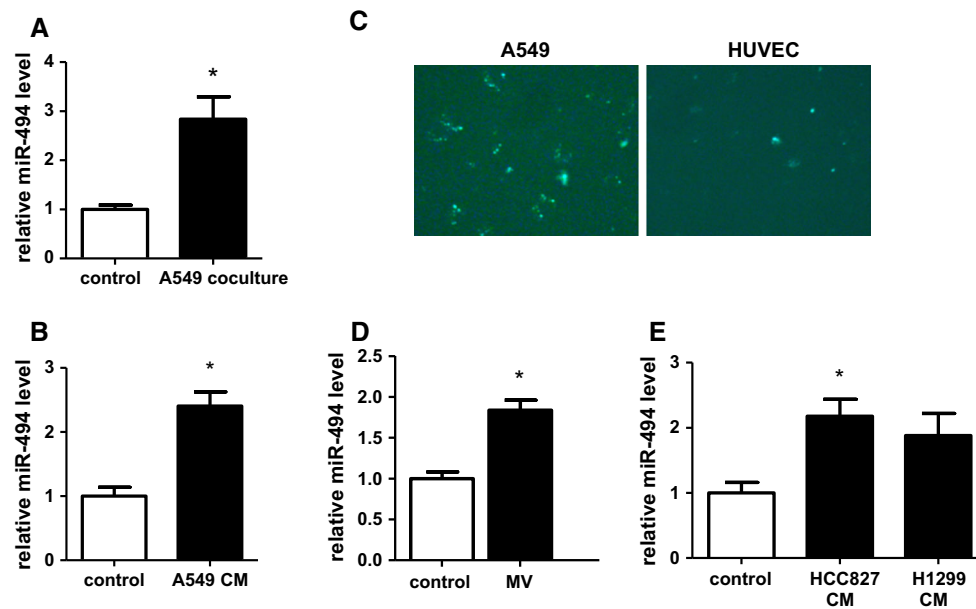


**Fig. 3** Delivery of the tumor cell-derived miR-494 to ECs via MVs. **a** HUVECs were co-cultured with A549 cells (inserted in upper well) or with HUVECs as control for 24 h. RNA samples were isolated from ECs cultured in the lower wells. The level of mature miR-494 was assessed with Taqman qRT-PCR and normalized to that of U6. **b** HUVECs were treated with CM from A549 or HUVECs (as control) for 24 h. **c** HUVECs were incubated with the conditioned media from A549 cells transfected with FAM-tagged miR494 or from

HUVECs as a control for 12 h. Fluorescence microscopy image of A549 transfected with FAM-tagged miR-494 and HUVECs incubated with MVs bearing FAM-tagged miR-494 for 12 h. **d** HUVECs were incubated with or without MVs isolated from A549 for 12 h before RNA isolation. **e** HUVECs were treated with the CM from HCC827, H1299 cells or HUVECs (control) for 24 h. The levels of mature miR-494 transcript were expressed as fold of controls. \* $P < 0.05$  versus control ( $n = 3$ )

the activation of Akt/eNOS pathway, which is negatively regulated by PTEN level and positively involved in angiogenesis process. As shown in Fig. 2b, the phosphorylations of Akt and eNOS were increased in ECs treated with miR-494 mimic and decreased in those treated with miR-494 inhibitor.

To test whether miR-494-induced cell migration is dependent on Akt/eNOS pathway, we used LY294002 and L-NAME to inhibit Akt and eNOS activities, respectively. As expected, miR-494-induced phosphorylation of Akt and eNOS was significantly suppressed with the treatment of LY294002. Furthermore, treatment of Akt inhibitor LY294002 or the eNOS inhibitor L-NAME abolished the effects of miR-494 in cell migration (Fig. 2c) and formation of tube-like structure in ECs (Fig. 2d).

### Tumor cells increased miR-494 in ECs via microvesicle-mediated delivery

As miR-494 promoted endothelial migration and tube formation in vitro, we used a tumor–endothelial co-culture system to examine the role of miR-494 in tumor angiogenesis. Co-culture with A549 significantly increased the level of mature miR-494 in ECs (Fig. 3a). Moreover, conditioned

medium from A549 cells had a similar effect (Fig. 3b). These results suggested that A549-secreted factors might contribute to the increased miR-494 in ECs. We treated HUVECs with several factors including VEGF, bFGF, ET-1 and TNF $\alpha$ , which are reported and involved in tumor angiogenesis process. However, none of these factors were able to increase miR-494 in ECs (Supplemental Fig. 1A).

Thus, we tested the possibility that the increased miR-494 was resulted from the delivery from the co-cultured A549 cells. Firstly, we found that the level of miR-494 primary transcript, pri-miR-494, was not changed in ECs treated with A549-conditioned medium or after co-culture with A549 (Supplemental Fig. 1B and C). Next, we transfected a FAM fluorescence-labeled synthetic miR-494 into A549 cells and used the conditioned medium to treat HUVECs for 6 h and then washed the HUVECs with PBS for three times. Fluorescence microscopy demonstrated the transfer of the labeled miR-494 from A549 cells into ECs (Fig. 3c). In addition, HUVECs were treated with the microvesicles extracted from the A549-conditioned medium. Real-time PCR showed that the microvesicles also increased the miR-494 level in ECs (Fig. 3d). Importantly, treatment with conditioned media from H1299 and HCC 827, the other lung cancer cells, similarly increased miR-

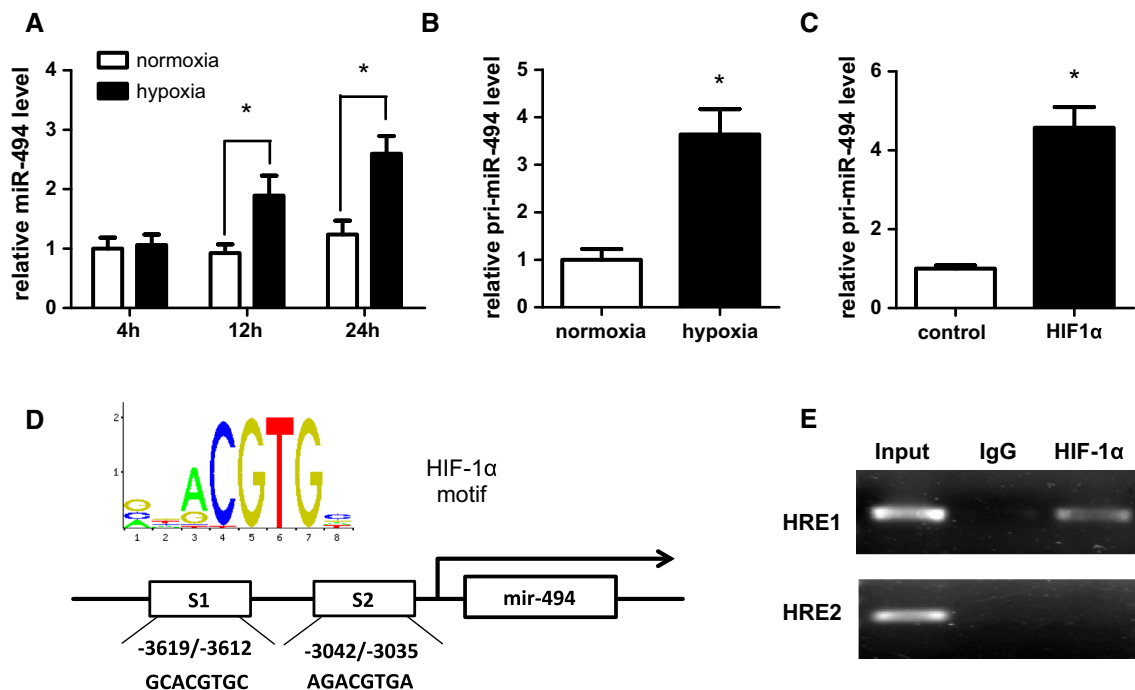


**Fig. 4** Hypoxia induced expression of miR-494 in A549 cells. **a** Levels of miR-494 were detected in A549 cells after the exposure to hypoxia (1 % O<sub>2</sub>) or normoxic control for the indicated time period. **b** Relative levels of pri-miR-494 in A549 cells after exposure to hypoxia or normoxia for 24 h. **c** The pri-miR-494 levels in A549 cells were detected 24 h after transfection with a HIF-1α expression plasmid or the vector control. \**P* < 0.05 versus control (*n* = 3). **d** The diagram depicts the two putative HIF-1α motifs located in the

5'-flanking region of the human miR-494 gene. **e** A549 cells were treated with hypoxia for 12 h and subjected to ChIP assays with antibodies against HIF-1α or IgG (as a control) followed by the PCR amplifications using primers flanking the two putative HREs. HRE1 is the binding site located at -3619/-3612 (S1) and HRE2 is located at -3042/-3035 (S2). DNA samples without immunoprecipitation were used as positive control (input)

494 in HUVECs (Fig. 3e). Functionally, A549-conditioned medium significantly accelerated EC migration. This effect was attenuated in ECs transfected with miR-494 inhibitor (Fig. 1e). Taken together, these results indicated that miR-494 is a pro-angiogenic signal delivered into ECs from cancer cells.

#### Hypoxia induces miR-494 expression via a HIF-1α-mediated mechanism

Hypoxia is a primary factor to stimulate tumor angiogenesis. We treated A549 cells with chronic hypoxia condition (1 % oxygen) and found that the levels of both mature and primary miR-494 were increased in A549 cells after 24 h compared with normoxic group (Fig. 4a, b), indicating that miR-494 was transcriptionally upregulated by hypoxia.

In order to explore the mechanism underlying the hypoxia induction of miR-494, we overexpressed HIF-1α in A549 cells and found that the expression of pri-miR-494 was induced by HIF-1α (Fig. 4c). Bioinformatic analysis using JASPAR (<http://jaspar.genereg.net>) predicted two putative binding sites for HIF-1α in 5'-flanking region of

the human miR-494 gene (Fig. 4d). ChIP assay confirmed the HIF-1α binding to the distal site (Fig. 4e).

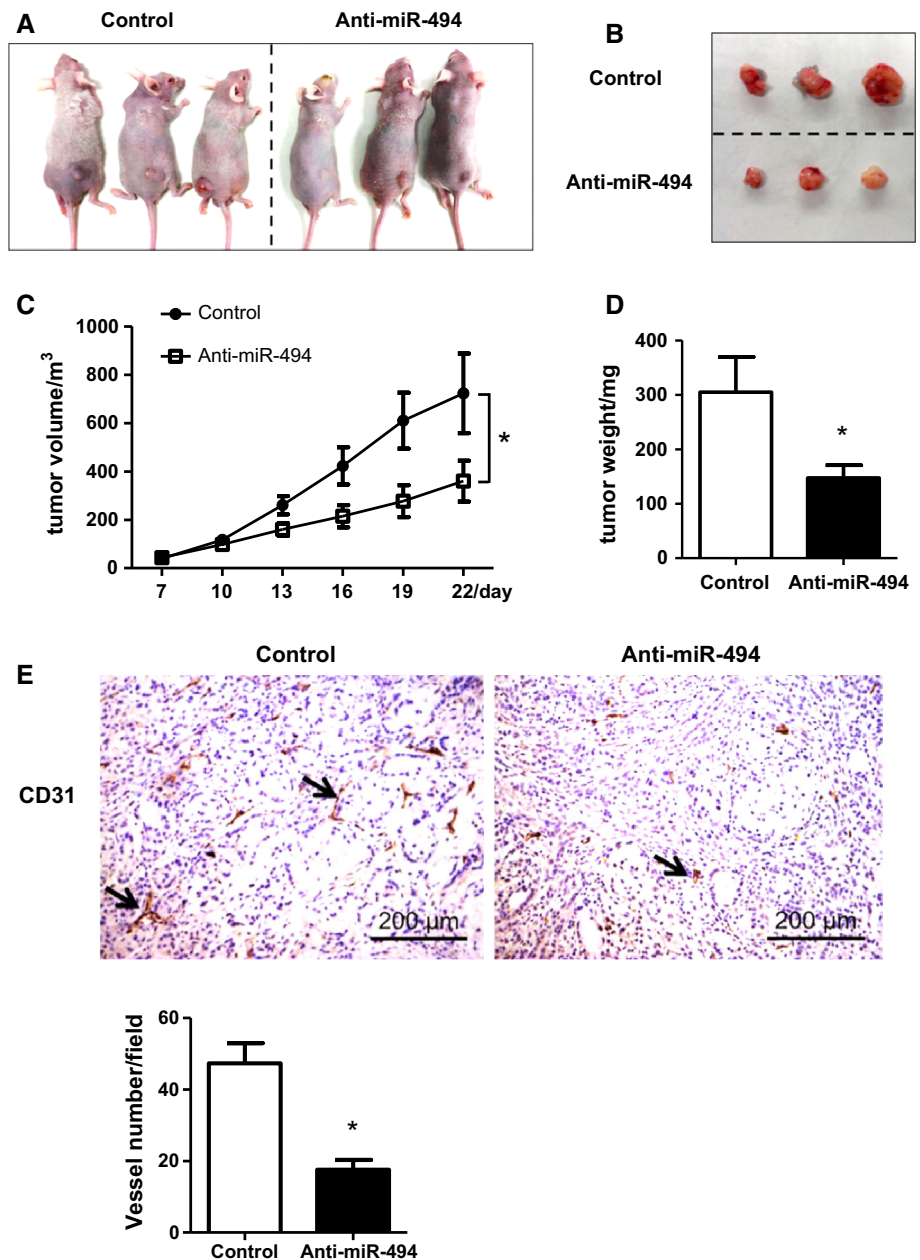
#### miR-494 inhibits tumor angiogenesis in vivo

We used a xenograft mouse model to examine the effect of miR-494 inhibitor on tumor angiogenesis. In A549 cells-inoculated nude mice, intratumoral administration of antagomiR-494 significantly inhibited the tumor growth (Fig. 5a–d). Most importantly, angiogenesis was suppressed in the antagomiR-494 treated group, as assessed by CD31 immunostaining (Fig. 5e). It is thus indicated that targeting miR-494 is a potential anti-angiogenic strategy for cancer therapy.

#### Discussion

In the present study, we demonstrated for the first time that miR-494 is an important tumor-derived microRNA to promote tumor angiogenesis. MiR-494 is upregulated by hypoxia stimuli in tumor cells via a HIF-1α-mediated transcriptional regulation. This upregulated miR-494 was

**Fig. 5** AntagomiR against miR-494 inhibited tumor angiogenesis and growth. **a** A549 cells were inoculated subcutaneously in the flank site of BALB/c nude mice. Mice bearing A549 tumors were intratumorally injected with the miR-494 antagomiR or scramble control on day 8 and 15. After 3 weeks, mice were killed for examination. **b** The tumor xenografts excised from mice treated with miR-494 antagomiR or control. **c** Tumor volumes were measured by every 3 days starting from the day before the treatment. **d** The weights of the excised tumors. **e** Tumor angiogenesis was assessed with immunohistochemical staining using an antibody against CD31. Endothelia (*arrow*) were stained *dark brown*. Blood vessels were quantified on two sections (six random fields/section) from each mouse (six mice per group). \**P* < 0.05 versus control. (Color figure online)

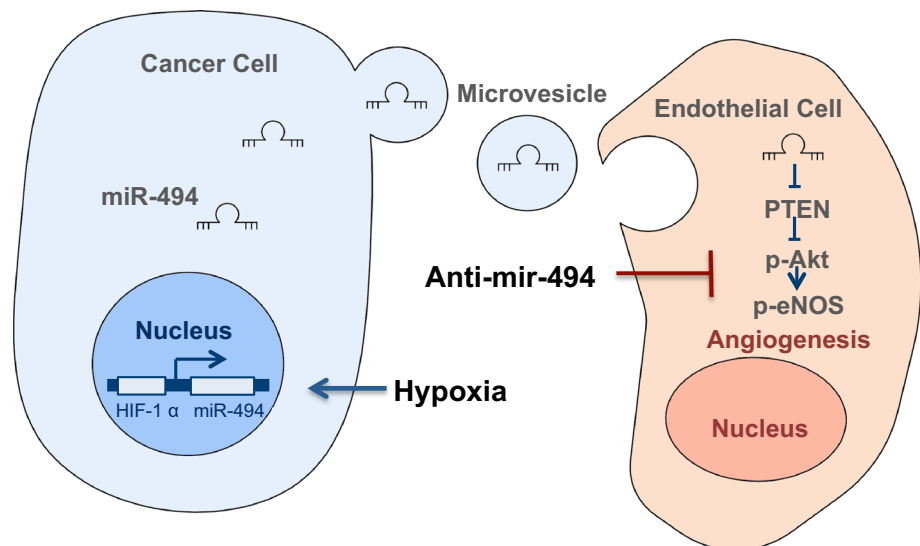


firstly secreted from tumor cells into microenvironment and delivered into ECs via MVs, then downregulated PTEN and activated Akt/eNOS pathway in ECs, finally exacerbated tumor development by promoting angiogenesis (Fig. 6).

Our study described a novel pathway that tumor cells facilitate angiogenesis via secretion of MVs containing miR-494 into the surrounding microenvironment. Mir-494 packed in MVs can be uptaken by recipient ECs and consequently promotes the angiogenesis. Tumor-derived MVs have been shown to shape the tumor and metastatic environment [22–24]. Tumor cells can use MVs as a cargo

to transfer angiogenic factors, including proteins and microRNAs [25]. MVs released from human renal cancer stem cells triggered angiogenesis and formed a pro-metastatic niche in lungs [18]. Recently, it has been reported that miR-1245 in colorectal cancer cell-derived MVs promoted angiogenesis in vitro [26]. In this study, we found that the tumor-derived miR-494 was delivered *en route* MVs into ECs to promote angiogenesis. This notion is supported by several lines of evidence: (1) Mature but not the primary form of miR-494 was elevated in ECs co-cultured with three different lung cancer cell lines; (2) MVs extracted from the tumor cells-conditioned media also

**Fig. 6** Tumor-derived miR-494 conveys a pro-angiogenic signal. In tumor (NSCLC) cells, hypoxia induced the expression of miR-494 by HIF-1 $\alpha$ -mediated transcription. The miR-494 was secreted and delivered, via MVs, into residential ECs. Suppression of PTEN by miR-494 activated Akt/eNOS pathway and mobilized EC migration and angiogenesis, which reshaped a proliferative microenvironment. The miR-494 antagomiR blocked angiogenesis and, thus, effectively inhibited tumor growth



increased the miR-494 level in ECs; (3) the pro-migratory capacity of the conditioned media on ECs was diminished by a specific inhibitor of miR-494. This finding provided a new insight into the MV-mediated pathway in the modulation of lung cancer microenvironment.

The pro-angiogenic capacity of miR-494 was mediated via the PTEN/Akt/eNOS axis. Targeting of PTEN by miR-494 was previously demonstrated in a bronchial epithelial cell line and cardiomyocytes [21, 27]. We found that miR-494 targeting of PTEN, a phosphatase of Akt kinase, led to an increased phosphorylation of Akt. As a result, eNOS activation mediated the pro-migratory effect. Moreover, the inhibition of Akt or eNOS abolished the pro-angiogenesis effect (Fig. 2c, d), establishing the importance of the Akt/eNOS pathway in mediating the effect of miR-494 on angiogenesis. Considering that Akt/eNOS pathway is regulated by many angiogenic factors such as VEGF, FGF or TGF- $\beta$  and its central role in angiogenesis [28], inhibition of PTEN by miR-494 would de-brake the Akt/eNOS activation and lead to a pro-angiogenic microenvironment in tumorous tissues.

The increased metabolic activity and oxygen consumption of rapidly proliferating tumor cells can produce a hypoxic tumor microenvironment, which drives angiogenesis [29]. Expression of miR-494 was induced in cancer cells upon the exposure to hypoxia (Fig. 4), suggesting that miR-494 is a hypoxia-responsive gene. We also demonstrated that miR-494 is a downstream target gene of HIF-1 $\alpha$  (Fig. 4), which is a transcriptional factor stabilized and translocated into the nucleus under hypoxic conditions. Previous study showed that HIF-1 $\alpha$  plays a pivotal role in the hypoxia response by activating a broad array of genes including VEGF, interleukin-8 and bFGF. A number of pro-angiogenic

microRNAs were known to be regulated by hypoxia [30–35]. For instance, miR-382 had been shown to be a target gene of HIF-1 $\alpha$  and regulated tumor angiogenesis in gastric cancer [36]. Moreover, the expression level of miR-494 could also be regulated by other transcription factors such as AP-1, which could bind to the promoter region of miR-494 gene to regulate its expression in NSCLC [37].

A most recent study found that the expression of miR-494 was significantly higher in the non-small lung cancer (NSCLC) lesions than that in normal adjacent lung tissues and positively associated with pathological TNM staging and lymph node metastasis. In addition, the increased miR-494 levels were negatively correlated with the survival probabilities, indicating that miR-494 may be an independent prognostic factor for NSCLC [38]. Moreover, previous studies suggested an oncogenic potential of miR-494 in lung cancers. In a transformed human bronchial epithelial cell line, inhibition of miR-494 decreased the malignancy of transformed cells induced by air pollutants benzo(a)pyrene diolepoxide (BPDE) and radon [27, 39]. In addition, activation of the mitogenic signaling pathways such as Erk1/2 increased the expression of miR-494, inducing tumor necrosis factor (TNF)-related apoptosis-inducing ligand (TRAIL) resistance in NSCLC [37]. Besides lung cancer, it was reported that, miR-494 might even act as a tumor suppressor by targeting c-myc in gastric cancer [40]. According to our in vivo xenograft experiments, intratumor administration of the miR-494 antagomiR effectively reduced angiogenesis, demonstrating a pathophysiological role of miR-494 in mediating the tumor-derived angiogenic signaling. Importantly, the tumor-suppressive effect of the antagomiR provided the proof of concept that the targeting miR-494 is a potential strategy for the angiogenesis-based tumor therapy.



**Acknowledgments** This work was supported by grants from the National Science Foundation of China (#30881220108005, 31430045 and 81470373) and the Provincial Office of Science and Technology, Shaanxi (2011KTCQ03-14).

**Conflict of interest** The authors declare no conflict of interest.

## References

- Bartel DP (2009) MicroRNAs: target recognition and regulatory functions. *Cell* 136(2):215–233. doi:10.1016/j.cell.2009.01.002
- Wang Y, Lee CG (2009) MicroRNA and cancer—focus on apoptosis. *J Cell Mol Med* 13(1):12–23. doi:10.1111/j.1582-4934.2008.00510.x
- Stenvang J, Petri A, Lindow M, Obad S, Kauppinen S (2012) Inhibition of microRNA function by anti-miR oligonucleotides. *Silence* 3(1):1. doi:10.1186/1758-907X-3-1
- Jones K, Nourse JP, Keane C, Bhatnagar A, Gandhi MK (2014) Plasma microRNA are disease response biomarkers in classical Hodgkin lymphoma. *Clin Cancer Res* 20(1):253–264. doi:10.1158/1078-0432.CCR-13-1024
- Ries J, Vairaktaris E, Agaimy A, Kintopp R, Baran C, Neukam FW, Nkenke E (2014) miR-186, miR-3651 and miR-494: potential biomarkers for oral squamous cell carcinoma extracted from whole blood. *Oncol Rep* 31(3):1429–1436. doi:10.3892/or.2014.2983
- Lim L, Balakrishnan A, Huskey N, Jones KD, Jodari M, Ng R, Song G, Riordan J, Anderton B, Cheung ST, Willenbring H, Dupuy A, Chen X, Brown D, Chang AN, Goga A (2014) MicroRNA-494 within an oncogenic microRNA megacluster regulates G1/S transition in liver tumorigenesis through suppression of mutated in colorectal cancer. *Hepatology* 59(1):202–215. doi:10.1002/hep.26662
- Liu Y, Lai L, Chen Q, Song Y, Xu S, Ma F, Wang X, Wang J, Yu H, Cao X, Wang Q (2012) MicroRNA-494 is required for the accumulation and functions of tumor-expanded myeloid-derived suppressor cells via targeting of PTEN. *J Immunol* 188(11):5500–5510. doi:10.4049/jimmunol.1103505
- Weis SM, Cheresh DA (2011) Tumor angiogenesis: molecular pathways and therapeutic targets. *Nat Med* 17(11):1359–1370. doi:10.1038/nm.2537
- Zhang Y, Yang P, Wang XF (2014) Microenvironmental regulation of cancer metastasis by miRNAs. *Trends Cell Biol* 24(3):153–160. doi:10.1016/j.tcb.2013.09.007
- Wang X, Fang X, Zhou J, Chen Z, Zhao B, Xiao L, Liu A, Li YS, Shyy JY, Guan Y, Chien S, Wang N (2013) Shear stress activation of nuclear receptor PXR in endothelial detoxification. *Proc Natl Acad Sci USA* 110(32):13174–13179. doi:10.1073/pnas.1312065110
- Wang N, Verna L, Hardy S, Zhu Y, Ma KS, Birrer MJ, Stemmerman MB (1999) c-Jun triggers apoptosis in human vascular endothelial cells. *Circ Res* 85(5):387–393
- Leung EL, Fiscus RR, Tung JW, Tin VP, Cheng LC, Sihoe AD, Fink LM, Ma Y, Wong MP (2010) Non-small cell lung cancer cells expressing CD44 are enriched for stem cell-like properties. *PLoS ONE* 5(11):e14062. doi:10.1371/journal.pone.0014062
- Szot CS, Buchanan CF, Freeman JW, Rylander MN (2013) In vitro angiogenesis induced by tumor-endothelial cell co-culture in bilayered, collagen I hydrogel bioengineered tumors. *Tissue Eng Part C Methods* 19(11):864–874. doi:10.1089/ten.TEC.2012.0684
- Zhu TS, Costello MA, Talsma CE, Flack CG, Crowley JG, Hamm LL, He X, Hervey-Jumper SL, Heth JA, Muraszko KM, DiMeco F, Vescovi AL, Fan X (2011) Endothelial cells create a stem cell niche in glioblastoma by providing NOTCH ligands that nurture self-renewal of cancer stem-like cells. *Cancer Res* 71(18):6061–6072. doi:10.1158/0008-5472.CAN-10-4269
- Tang Z, Wang Y, Fan Y, Zhu Y, Chien S, Wang N (2008) Suppression of c-Cbl tyrosine phosphorylation inhibits neointimal formation in balloon-injured rat arteries. *Circulation* 118(7):764–772. doi:10.1161/CIRCULATIONAHA.107.761932
- Liu Y, Tian XY, Mao G, Fang X, Fung ML, Shyy JY, Huang Y, Wang N (2012) Peroxisome proliferator-activated receptor-gamma ameliorates pulmonary arterial hypertension by inhibiting 5-hydroxytryptamine 2B receptor. *Hypertension* 60(6):1471–1478. doi:10.1161/HYPERTENSIONAHA.112.198887
- Liu W, Li JJ, Liu M, Zhang H, Wang N (2015) PPAR-gamma promotes endothelial cell migration by inducing the expression of Sema3g. *J Cell Biochem* 116(4):514–523. doi:10.1002/jcb.24994
- Grange C, Tapparo M, Collino F, Vitillo L, Damasco C, Deregibus MC, Tetta C, Bussolati B, Camussi G (2011) Microvesicles released from human renal cancer stem cells stimulate angiogenesis and formation of lung premetastatic niche. *Cancer Res* 71(15):5346–5356. doi:10.1158/0008-5472.CAN-11-0241
- Nagasu T, Yoshimatsu K, Rowell C, Lewis MD, Garcia AM (1995) Inhibition of human tumor xenograft growth by treatment with the farnesyl transferase inhibitor B956. *Cancer Res* 55(22):5310–5314
- Bao S, Wu Q, Sathornsumetee S, Hao Y, Li Z, Hjelmeland AB, Shi Q, McLendon RE, Bigner DD, Rich JN (2006) Stem cell-like glioma cells promote tumor angiogenesis through vascular endothelial growth factor. *Cancer Res* 66(16):7843–7848. doi:10.1158/0008-5472.CAN-06-1010
- Wang X, Zhang X, Ren XP, Chen J, Liu H, Yang J, Medvedovic M, Hu Z, Fan GC (2010) MicroRNA-494 targeting both proapoptotic and antiapoptotic proteins protects against ischemia/reperfusion-induced cardiac injury. *Circulation* 122(13):1308–1318. doi:10.1161/CIRCULATIONAHA.110.964684
- Al-Nedawi K, Meehan B, Rak J (2009) Microvesicles: messengers and mediators of tumor progression. *Cell Cycle* 8(13):2014–2018
- Muralidharan-Chari V, Clancy JW, Sedgwick A, D'Souza-Schorey C (2010) Microvesicles: mediators of extracellular communication during cancer progression. *J Cell Sci* 123(Pt 10):1603–1611. doi:10.1242/jcs.064386
- Valenti R, Huber V, Iero M, Filipazzi P, Parmiani G, Rivoltini L (2007) Tumor-released microvesicles as vehicles of immunosuppression. *Cancer Res* 67(7):2912–2915. doi:10.1158/0008-5472.CAN-07-0520
- D'Souza-Schorey C, Clancy JW (2012) Tumor-derived microvesicles: shedding light on novel microenvironment modulators and prospective cancer biomarkers. *Genes Dev* 26(12):1287–1299. doi:10.1101/gad.192351.112
- Yamada N, Tsujimura N, Kumazaki M, Shinohara H, Taniguchi K, Nakagawa Y, Naoe T, Akao Y (2014) Colorectal cancer cell-derived microvesicles containing microRNA-1246 promote angiogenesis by activating Smad 1/5/8 signaling elicited by PML down-regulation in endothelial cells. *Biochim Biophys Acta* 1839(11):1256–1272. doi:10.1016/j.bbagr.2014.09.002
- Liu L, Jiang Y, Zhang H, Greenlee AR, Han Z (2010) Overexpressed miR-494 down-regulates PTEN gene expression in cells transformed by anti-benzo(a)pyrene-trans-7,8-dihydrodiol-9,10-epoxide. *Life Sci* 86(5–6):192–198. doi:10.1016/j.lfs.2009.12.002
- Shiojima I, Walsh K (2002) Role of Akt signaling in vascular homeostasis and angiogenesis. *Circ Res* 90(12):1243–1250
- Liao D, Johnson RS (2007) Hypoxia: a key regulator of angiogenesis in cancer. *Cancer Metastasis Rev* 26(2):281–290. doi:10.1007/s10555-007-9066-y
- Voellenkle C, Rooij J, Guffanti A, Brini E, Fasanaro P, Isaia E, Croft L, David M, Capogrossi MC, Moles A, Felsani A, Martelli

- F (2012) Deep-sequencing of endothelial cells exposed to hypoxia reveals the complexity of known and novel microRNAs. *RNA* 18(3):472–484. doi:[10.1261/rna.027615.111](https://doi.org/10.1261/rna.027615.111)
31. Cha ST, Chen PS, Johansson G, Chu CY, Wang MY, Jeng YM, Yu SL, Chen JS, Chang KJ, Jee SH, Tan CT, Lin MT, Kuo ML (2010) MicroRNA-519c suppresses hypoxia-inducible factor-1alpha expression and tumor angiogenesis. *Cancer Res* 70(7):2675–2685. doi:[10.1158/0008-5472.CAN-09-2448](https://doi.org/10.1158/0008-5472.CAN-09-2448)
32. Puissegur MP, Mazure NM, Bertero T, Pradelli L, Grosso S, Robbe-Sermesant K, Maurin T, Lebrigand K, Cardinaud B, Hofman V, Fourre S, Magnone V, Ricci JE, Pouyssegur J, Gounon P, Hofman P, Barbry P, Mari B (2011) miR-210 is overexpressed in late stages of lung cancer and mediates mitochondrial alterations associated with modulation of HIF-1 activity. *Cell Death Differ* 18(3):465–478. doi:[10.1038/cdd.2010.119](https://doi.org/10.1038/cdd.2010.119)
33. Ghosh G, Subramanian IV, Adhikari N, Zhang X, Joshi HP, Basi D, Chandrashekar YS, Hall JL, Roy S, Zeng Y, Ramakrishnan S (2010) Hypoxia-induced microRNA-424 expression in human endothelial cells regulates HIF-alpha isoforms and promotes angiogenesis. *J Clin Invest* 120(11):4141–4154. doi:[10.1172/JCI42980](https://doi.org/10.1172/JCI42980)
34. Chan YC, Khanna S, Roy S, Sen CK (2011) miR-200b targets Ets-1 and is down-regulated by hypoxia to induce angiogenic response of endothelial cells. *J Biol Chem* 286(3):2047–2056. doi:[10.1074/jbc.M110.158790](https://doi.org/10.1074/jbc.M110.158790)
35. Liu LZ, Li C, Chen Q, Jing Y, Carpenter R, Jiang Y, Kung HF, Lai L, Jiang BH (2011) MiR-21 induced angiogenesis through AKT and ERK activation and HIF-1alpha expression. *PLoS ONE* 6(4):e19139. doi:[10.1371/journal.pone.0019139](https://doi.org/10.1371/journal.pone.0019139)
36. Seok JK, Lee SH, Kim MJ, Lee YM (2014) MicroRNA-382 induced by HIF-1alpha is an angiogenic miR targeting the tumor suppressor phosphatase and tensin homolog. *Nucleic Acids Res* 42(12):8062–8072. doi:[10.1093/nar/gku515](https://doi.org/10.1093/nar/gku515)
37. Romano G, Acunzo M, Garofalo M, Di Leva G, Cascione L, Zanca C, Bolon B, Condorelli G, Croce CM (2012) MiR-494 is regulated by ERK1/2 and modulates TRAIL-induced apoptosis in non-small-cell lung cancer through BIM down-regulation. *Proc Natl Acad Sci USA* 109(41):16570–16575. doi:[10.1073/pnas.1207917109](https://doi.org/10.1073/pnas.1207917109)
38. Wang J, Chen H, Liao Y, Chen N, Liu T, Zhang H, Zhang H (2015) Expression and clinical evidence of miR-494 and PTEN in non-small cell lung cancer. *Tumor Biol*. doi:[10.1007/s13277-015-3416-0](https://doi.org/10.1007/s13277-015-3416-0)
39. Cui FM, Li JX, Chen Q, Du HB, Zhang SY, Nie JH, Cao JP, Zhou PK, Hei TK, Tong J (2013) Radon-induced alterations in microRNA expression profiles in transformed BEAS2B cells. *J Toxicol Environ Health A* 76(2):107–119. doi:[10.1080/15287394.2013.738176](https://doi.org/10.1080/15287394.2013.738176)
40. He W, Li Y, Chen X, Lu L, Tang B, Wang Z, Pan Y, Cai S, He Y, Ke Z (2014) miR-494 acts as an anti-oncogene in gastric carcinoma by targeting c-myc. *J Gastroenterol Hepatol* 29(7):1427–1434. doi:[10.1111/jgh.12558](https://doi.org/10.1111/jgh.12558)